

# Influence of reduced VAV flow settings on indoor thermal comfort in an office space

Kavita Gangiseti<sup>1</sup>, David E. Claridge<sup>1</sup>, Jelena Srebric<sup>2</sup>, Mitchell T. Paulus<sup>1</sup> (✉)

1. Texas A&M University, 402 Harvey Mitchell Pkwy S, College Station, TX 77845, USA

2. University of Maryland, 3143 Glenn L. Martin Hall, College Park, MD 20742, USA

## Abstract

The air temperature distribution in a space with reduced diffuser flow rates and heat loads was studied using simulation. Computational fluid dynamics (CFD) was used to analyze the room air distribution from a side wall diffuser at the design flow rate, and the results were validated with experimental data. CFD was used to predict occupant discomfort under a range of reduced diffuser flow rates. It was found for diffuser flow rates above 30% of the design flow rate that the temperature influence from the jet was minimal. At these flow rates, there was nearly a uniform temperature distribution in the occupied zone. The predicted maximum value of percentage of dissatisfied occupants within the space began to increase for diffuser flow rates below 30% of the design flow rate. The percent dissatisfaction at 1 m room height was greater than 25% for the lowest diffuser flow rate tested (15% of the design flow rate) directly under the diffuser, which was the highest of the test cases, but was 5% or less throughout more than 90% of the room. In contrast, at the higher flow rates, the percent dissatisfied index was 5% or less in only 60%–80% of the room due to increased velocity. Evidence of dumping was already found at the traditional minimum flow rate setting of 30% of design, and so there would be little harm in reducing the minimum flow rate further. Reducing the flow rate below 30% of design just moved the location of the dumping closer to the diffuser. For very low diffuser flow rates (below 30% of the design flow rate), it is recommended that desks be placed away from the supply diffuser to avoid discomfort. Overall, the simulation results indicate that uniform temperatures are maintained in the room at flow rates as low as 15% of design except immediately under the diffuser. This suggests that the VAV minimum flow rates can be set below 30% of design flow as long as the diffuser is at least 1 m from an occupant's position.

## 1 Introduction

The movement of air through interior spaces of a building represents space or room air diffusion. Air enters the room/space through a supply outlet to increase thermal comfort and to improve indoor air quality. Numerical prediction of airflow patterns has been a research area for several decades. By 1980, it was possible to predict the flow field in large domains with relatively small openings using computational fluid dynamics (CFD) (Gosman et al. 1980).

In recent years, CFD has gained popularity as a design and analytical tool because it offers an engineer the ability

to visualize the air movement inside the room. It enables one to predict discrete velocity and temperature values and their distributions in a space. It also allows an engineer to change parameters such as flow rates, inlet temperature, heat loading, occupancy, and to predict the impact of these design changes on indoor climate and energy consumption in actual buildings. Thermal comfort can be predicted in a variety of places such as theatres (Cheong et al. 2003), arenas (Stamou et al. 2008), buses (Riachi and Clodic 2014), and kitchens (Simone et al. 2013) using CFD. Various air conditioning methods have also been studied. As an example, Kajiya et al. (2011) reproduced the human environment from a floor

## Keywords

CFD,  
thermal comfort,  
draught,  
diffusers,  
turbulence

## Article History

Received: 9 March 2015

Revised: 2 September 2015

Accepted: 11 September 2015

© Tsinghua University Press and  
Springer-Verlag Berlin Heidelberg  
2015

heated room with CFD.

Variable-air-volume distribution systems vary the flow rate of air into a room while supplying air at a constant temperature to maintain the temperature in the space until the required flow drops to a minimum flow set point. For lower cooling loads in the space, the temperature of the supply air is increased, typically by inefficient reheat, to maintain comfort at this minimum flow rate. The minimum flow rate is typically set at 30% to 50% of the design flow as seen in Fig. 1. Lower flow rates may cause discomfort due to cold spots in the room caused by “dumping”, where the cold air will fall directly below the diffuser and cause discomfort for the occupants or that there will be “hot” spots because the air does not mix well. These temperature differences increase the effective draft temperature in local areas. This paper explores the impact of diffuser flow rates on comfort in an office space using CFD simulations.

A recent ASHRAE research project (RP-1515) investigated thermal comfort concerns regarding reducing the minimum airflow from overhead diffusers (Arens et al. 2012). The investigators found no effect in occupant responses from thermal comfort surveys when the VAV terminal box minimum flow rate was set to less than 20% of the maximum. Furthermore, the investigators found that the reduced minimum diffuser flow rate not only saved energy, but also significantly reduced occupant discomfort in the summer from over-cooling, an issue discussed in detail by Mendell and Mirer (2009). Noh et al. (2007) also reached a similar conclusion that thermal comfort was not affected by their variation in the discharge airflow.

This study numerically examines thermal comfort in a small office space with different air supply rates. The space dimensions and layout correspond to the setup in an environmental chamber with published experimental data available, which allows for validation of the CFD simulations

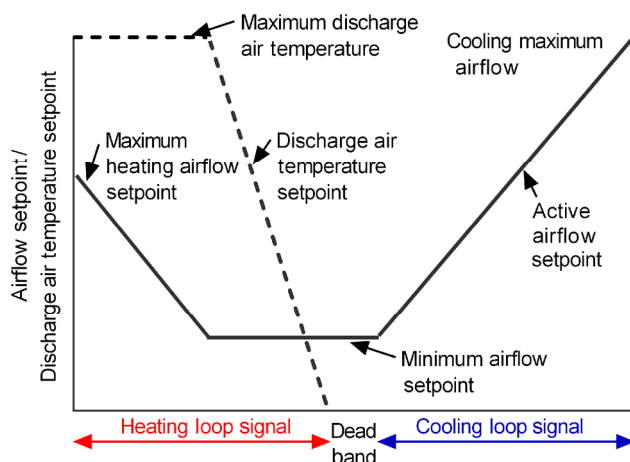


Fig. 1 Typical dual maximum VAV terminal box control with reheat, adapted with permission (Arens et al. 2012)

(Srebric and Chen 2001, 2002; Chen and Moser 1991). The current study used this setup for a baseline simulation, and further validated the baseline simulation results by comparing them to the measured maximum velocity, distribution of velocity, and temperature in the room. Furthermore, this study investigated the influence of different physical and numerical parameters on the baseline results. Specifically, this study modified the diffuser inlet angle, the grid size, the turbulence model, and the radiative fluxes in the room air simulations. The values of these parameters that provided the best agreement between the simulated and measured data were used for simulations with the reduced diffuser flow rates.

Once the baseline simulation was validated, further analysis was carried out with the reduced diffuser flow rates. The supply flow rates were reduced in steps from the design flow rate (100%) to 15% of the design flow rate. The intent was to predict the draft, jet momentum, air velocity, and temperature distribution inside the room. Finally, the draft and temperature distribution in the occupied zone was studied in detail to determine the impact of reduced flow rates and loading on comfort in the space. This work uses a validated CFD model to theoretically examine the draught risk from a sidewall diffuser, and thus provide a theoretical basis for the findings by Arens et al. (2012) that reducing the minimum diffuser flow rates for this type of office setup does not negatively affect the overall thermal comfort for the space.

## 2 Methodology

This study adopted the thermal comfort model defined by draft as the criteria for evaluation of indoor thermal conditions under different supply flow rates. The accuracy of thermal comfort predictions strongly depends on the supply diffuser setup in the CFD simulations. Therefore, the thermal comfort definition and supply diffuser boundary conditions are important parts of the research methodology.

### 2.1 Thermal comfort based on draft

Thermal comfort is defined as the condition of mind that expresses satisfaction with the thermal environment (ASHRAE 2013). Factors that influence comfort and are controllable by the building operator include the air temperature, humidity, and velocity. Factors that are not controllable by the building operator include activity level, clothing, and personal preference. There are several recent review papers from the past 5 years covering research in the field of thermal comfort (Rupp et al. 2015; Yang et al. 2014; Kwong et al. 2014; Taleghani et al. 2013; De Dear et al. 2013; Cheng et al. 2012; Carlucci and Pagliano 2012; Djongyong

et al. 2010). From these reviews, there has been a shift towards adaptive thermal comfort models and significant benefits shown from occupants controlling their own indoor environment. Air movement has been perceived in a more positive way, especially when tied to occupant control under increased indoor air temperatures.

Draft is one possible negative component of air movement, when there is undesired local cooling on the body. Fanger and Christensen (1986) determined a relationship for the percentage of population feeling draft when exposed to a given mean air velocity at the neck. Fanger et al. (1988) investigated the effect of turbulence intensity on the sensation of draft. Turbulence intensity significantly affects draft sensation, as predicted by Eq. (1).

$$PD = (34 - T_a)(V - 0.05)^{0.62} [0.37(V)(Tu) + 3.14] \quad (1)$$

PD is the percent dissatisfied,  $T_a$  is the dry-bulb air temperature (°C), and  $V$  is the air velocity magnitude (m/s).  $Tu$  is the turbulence intensity in percentage, defined as

$$Tu = \frac{\sqrt{k}}{1.1V} \quad (2)$$

where  $k$  is the turbulence kinetic energy. This model can be used to quantify draft risk in spaces and to develop air distribution systems with a low draft risk.

The validity of Fanger's draught model was assessed in depth by Charles (2003). A noted limitation of the model is that in recent studies people have been shown to tolerate higher air velocities if given personal control (Cândido et al. 2010; Arens et al. 1998; Kubo et al. 1997; Fountain et al. 1994) and that more air movement, possibly above current standards, may be desired in "neutral" or "slightly warm" conditions (Zhang et al. 2007). Importantly, these studies concluded that Fanger's draught model is applicable to occupants performing sedentary activities under conditions near or at thermal neutrality without personal control of ventilation.

## 2.2 Diffuser boundary conditions

Proper specification of diffuser boundary conditions is essential for room air modeling with CFD. There are two major difficulties in simulating the diffuser. The first difficulty is the size of the diffuser geometry, which is small compared to the size of the room. The second difficulty is the complex physics of the transitional flow regime with heat transfer driven by convection. As a result, a diffuser requires a large number of nodes or grid cells to model the flow in the region near the diffuser outlet accurately. Therefore, it is important to capture the flow features in

front of a diffuser with a simpler model because there is an exponential increase in the computational time with the linear increase in the number of grid cells (Srebric and Chen 2002).

An extensive literature review presented different simplified methods for simulating diffuser boundary conditions (Srebric and Chen 2002; Srebric 2000). According to this study, diffuser analysis methods can be grouped into two basic categories including momentum modeling *at* the air supply devices and momentum modeling *in front of* the air supply devices.

The momentum modeling approach at the air supply device imposes initial jet momentum at the supply device. It is relatively easy to use and includes the basic model, wide slot model, and momentum method. The second category uses momentum downstream of the diffuser. It requires measurements and jet equations, and it includes the box model, prescribed velocity method, and diffuser specification method.

For the momentum modeling at the air supply devices, the basic model replaces the diffuser with a simple opening that has the same effective area as the original diffuser geometry (Heikkinen 1991a). The computed flow field looked similar to the one observed, but the maximum velocity was low and the jet spreading was not predicted well. Other studies showed that the jet profiles and decay are not predicted well, and that this model is not suitable for non-isothermal flows (Chen and Moser 1991; Ewert et al. 1991). The wide-slot model is a modification of the basic model. In this method, the same slot is chosen, but with a different aspect ratio (Heikkinen 1991a). The results showed that the mixing in the core and jet penetration was over predicted, making the wide-slot model ineffective. In the momentum method (Chen and Moser 1991), momentum and mass fluxes are decoupled at the diffuser boundary. The diffuser opening has the same gross area, mass flux, and momentum flux. A source for the momentum is introduced at the diffuser boundary to account for the actual discharge velocity. This method was validated with measured data for nozzle and displacement diffusers.

For the momentum modeling in front of the air supply devices, Nielsen (1992, 1989) proposed the box method in which an imaginary box is considered near the diffuser. The flow field inside the box is neglected. The measured velocity profiles are given as input on one side of the box, whereas the other sides use a free boundary condition with zero gradients for flow parameters. Results obtained from the box method were in good agreement with the measured data. The box method over predicted the maximum jet velocity and the velocity decay was slow.

The velocity model was proposed by Gosman et al. (1980) and further developed by Nielsen (1989). This method also

uses jet theory or measured data, but the space between the diffuser and profile location is included in the calculation. In this method, boundary conditions are given at a simple opening (as in the basic model) and in the flow field, similar to the box model. The velocities are taken either from theory or manufacturer specifications. Heikkinen (1991b) showed that the jet decay was well predicted, but the jet spread and maximum velocity were not. Skovgaard and Nielsen (1991) and Svidt (1994) showed that the results were in better agreement with the measured data than the basic model.

The diffuser specification model was proposed by Huo et al. (1996). This method is another modification of the box model. The model uses jet formulae for jet profiles, decay, and trajectories, and it does not require any measurements or manufacturer data. The use of jet formulae is advantageous when existing jet formulae are in the literature, but the model cannot be used to predict the flow distribution for several important special cases such as the partially attached jet and non-isothermal jets, since jet formulae are not available.

The models reviewed above have specific advantages and disadvantages. In this study, the momentum method at the supply outlet was selected from these proposed models to define the diffuser boundary condition for two particular reasons. It did not need experimental data (velocity, temperature and concentration profiles) that are often unavailable for diffusers, and it was simpler to implement and modify for different diffuser flow rates and discharge velocities.

### 3 Office model setup in CFD simulations

The baseline computational domain matched the experimental setup in the IEA Annex 20 project, and in particular Test Case B2, which was an experiment with forced convection and isothermal inlet airflow. More details regarding the experimental setup and measurement techniques can be found in the literature (Luo et al. 2004; Srebric 2000; Lemaire et al. 1993; Heikkinen 1991b). The lab setup consisted of a small empty office that was 4.2 m long, 3.6 m wide, and 2.5 m high, as shown in Fig. 2. It consisted of an air supply device (nozzle diffuser), an outlet, and a window. A HESCO type diffuser was employed, consisting of 84 small round nozzles arranged in four rows in an area of 0.71 m by 0.17 m. Each nozzle had a diameter of 11.8 mm and the total effective area for all the nozzles was 0.0008 m<sup>2</sup>. The flow direction of all the nozzles was adjusted to 40° upwards as shown in Fig. 2. The air entered with a flow rate of 3 ACH (0.0315 m<sup>3</sup>/s) at a supply temperature of 15 °C. Measurements were taken with an omnidirectional thermistor anemometer with 40 individually calibrated sensors.

Only half of the space was simulated because of the symmetry of the room. Heat flux penetrated through the

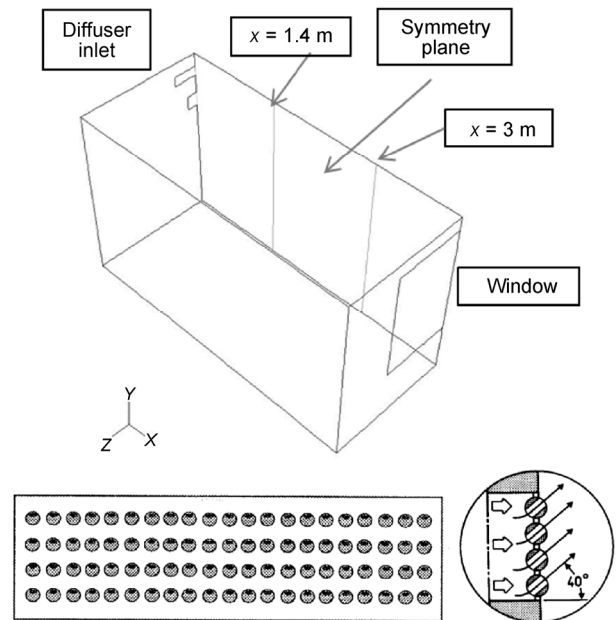


Fig. 2 Office layout (symmetry view) and diffuser orientation

window, which was initially assumed to have a surface temperature of 30 °C. Heat flux also entered by convection and radiation through each of the enclosure walls.

The working fluid was air. The fluid properties for air were held constant with air density equal to 1.225 kg/m<sup>3</sup> and viscosity equal to  $1.7894 \times 10^{-5}$  kg/(m·s). The solution was monitored at a point in the middle of the domain. Convergence was assumed when the residuals of each equation in the CFD program (ANSYS 2013) were below  $10^{-3}$  and when the average value of velocity magnitude at the monitored point became almost constant. A non-uniform structured mesh was used with a fine mesh near the walls and window. Grid sensitivity analysis on the mesh was performed, and the finalized mesh was used for analysis of different parameters.

#### 3.1 Boundary conditions at the inlet and outlet

From the literature review, the momentum method was selected for specifying the diffuser boundary conditions. With this method, the actual area of the diffuser was considered and the mass and momentum boundary conditions were decoupled. The inlet mass flow rate was given at the grille diffuser surface and a momentum source was defined near the inlet to account for the original supply velocity. The supply velocity was calculated from Eq. (3).

$$V_0 = \frac{\dot{m}}{\rho \times A_{\text{eff}}} \quad (3)$$

where  $\dot{m}$  is the mass flow rate of the diffuser,  $V_0$  is the actual supply velocity,  $\rho$  is the density of air, and  $A_{\text{eff}}$  is the effective

area of the diffuser that was calculated from the diffuser geometry.

The turbulence was specified using

$$k_0 = \frac{3}{2}(Tu \times V_0)^2 \quad (4)$$

$$\varepsilon_0 = \frac{C_\mu^{3/4} k_0^{3/2}}{l_0} \quad (5)$$

where  $V_0$  is the supply velocity,  $Tu$  is the turbulence intensity (assumed to be 10% based on previous literature (Srebric and Chen 2002)),  $C_\mu$  is an empirical constant,  $\varepsilon_0$  is the rate of dissipation of turbulent kinetic energy per unit mass, and  $l_0 = 0.1L$ , where  $L$  is the characteristic length of the diffuser.

Atmospheric pressure was given as the outlet boundary condition. The backflow turbulence was specified with intensity and length scale.

### 3.2 Boundary conditions at the wall surfaces

The surfaces enclosing the room were given no-slip wall boundary conditions. This indicated that the first fluid layer adjacent to the wall sticks to the wall and moves with the same velocity as the wall.

For the no-slip boundary condition, the properties of flow adjacent to the wall/boundary were used to predict the shear stress on the fluid at the wall,

$$\tau = \mu_{\text{eff}} \frac{\partial U}{\partial x} \quad (6)$$

$\tau$  is the shear stress,  $\mu_{\text{eff}}$  is the effective viscosity, and  $\frac{\partial U}{\partial x}$  is

the velocity gradient normal to the surface.

A surface to surface radiation model was used. In this model, it was assumed that the medium separating the walls of the room did not participate in the radiation process, which is a reasonable approximation for air.

## 4 Results

This section presents the CFD simulation model accuracy with different turbulence models, radiation models, and diffuser inlet angles. For the validated CFD model, this study further examined the impact of diffuser flow rates on the airflow field and temperature profiles as well as the thermal comfort.

### 4.1 Effect of turbulence model

In order to study the effect of turbulence models for predicting

the air velocities and temperatures inside the room, simulations were completed using four different turbulence models. The models were the  $k-\varepsilon$  model with low Reynolds number modification (LKE) proposed in the literature (Chen 1995), Renormalization-group (RNG)  $k-\varepsilon$  model, Reynolds stress model (RSM), and Transition  $k-\text{kl}-w$  model. The literature on these four turbulence models can be found in many textbooks on the subject of turbulence. The same non-uniform structured mesh was used for all the simulations in order to avoid grid diffusion errors. The results were plotted at the two poles ( $x = 1.4 \text{ m}$  and  $3 \text{ m}$ ) shown in Fig. 2.

The simulated results were compared with the experimental data available in the literature (Srebric and Chen 2002). The results of using the different turbulence models are shown in Fig. 3. LKE predicted velocities lower than the measured values in the near ceiling zone and higher velocities in the occupied zone, which was considered to be from the floor to 6 ft. or approximately 1.8 m. The RNG  $k-\varepsilon$  model had accurate predictions for velocities in the occupied zone, but predicted velocity higher than measured near the ceiling. The RSM and Transition  $k-\text{kl}-w$  models were more accurate. Furthermore, predicted temperature values with different turbulence models are compared with measured data in the bottom two plots of Fig. 3. LKE predicted the temperatures values approximately one degree lower than the measured values in the occupied zone. The RSM and RNG  $k-\varepsilon$  models accurately predicted temperature in the near ceiling region, but did not predict as well in the occupied zone. The transition  $k-\text{kl}-w$  model had the most accurate temperature predictions in the occupied zone. Overall, based on this experiment, the transition  $k-\text{kl}-w$  turbulence model is recommended for room air simulations.

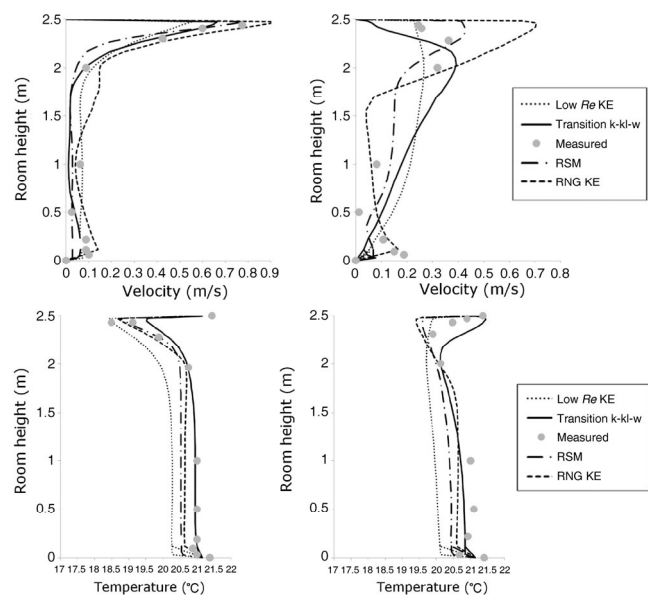


Fig. 3 Velocity and temperature profiles at  $x = 1.4 \text{ m}$  (left side) and  $3 \text{ m}$  (right side) in the symmetry plane

## 4.2 Effect of radiation model

Out of the three modes of heat transfer, convection is the dominant mode of heat transfer for air in a room. However, radiation should not be neglected for accurate predictions of room air temperatures. To study the effect of radiation, a model with radiation included and another model without radiation included were used. The predicted air temperature values were compared with measured temperature values as shown in Fig. 4. A surface to surface radiation model was used. In this model, it was assumed that the medium separating the walls of the room did not participate in the radiation process, which is a reasonable approximation for air. The emissivity of the walls was assumed equal to 0.75. The temperature values computed including the radiation model were in better agreement with the experimental measured data than without including radiation.

In practice, the simulation time increased when the radiation model was enabled. Hence, an alternate solution was proposed, which was to increase the wall temperature by 1 °C. The simulation results with adjusted wall temperatures were close to the results obtained by including the surface to surface radiation model. However, this approximation (increasing the wall temperature by 1 °C) only applied to this specific setup and would require adjustment if the inlet flow rate or inlet temperature were different. Additionally, the wall temperature has a fixed single value.

Overall, it is suggested to include a radiation model in room air simulations to accurately predict the air temperatures.

## 4.3 Effect of different diffuser inlet angles

To study the effect of the inlet angle of the diffuser jet on the jet momentum and room air velocities, the diffuser inlet angle was varied in the range of  $\pm 10^\circ$  of the original diffuser inlet angle ( $40^\circ$ ). Velocity profiles resulting from different jet angles were compared with the measured data at two different locations in the room as shown in Fig. 5. The velocities in the near ceiling region were affected more with the change in inlet angles than the velocities near the floor region. With a  $30^\circ$  inlet angle, the predicted jet velocity was less than measured near the ceiling region. The velocity increased as the jet angle was increased. With a  $50^\circ$  diffuser inlet angle, the velocity values seem to be the best fit in the occupied and near floor region. Velocities in most of the occupied zone (from  $y = 0.5$  m to  $y = 2$  m) increased as the diffuser angle was reduced.

This analysis showed that the diffuser inlet angle has an effect on the jet momentum (mainly in the ceiling region) and velocity distribution inside the room. The specification of a jet angle for the inlet diffuser boundary condition is

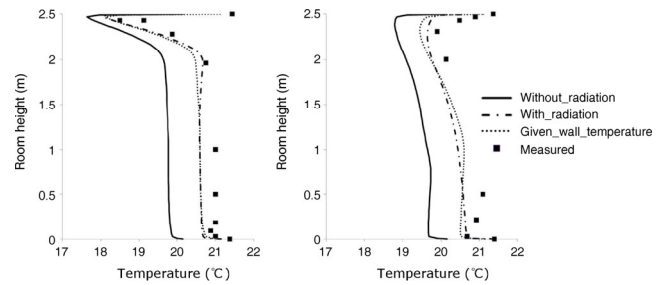


Fig. 4 Temperature profiles at  $x = 1.4$  m (left) and  $3$  m (right)

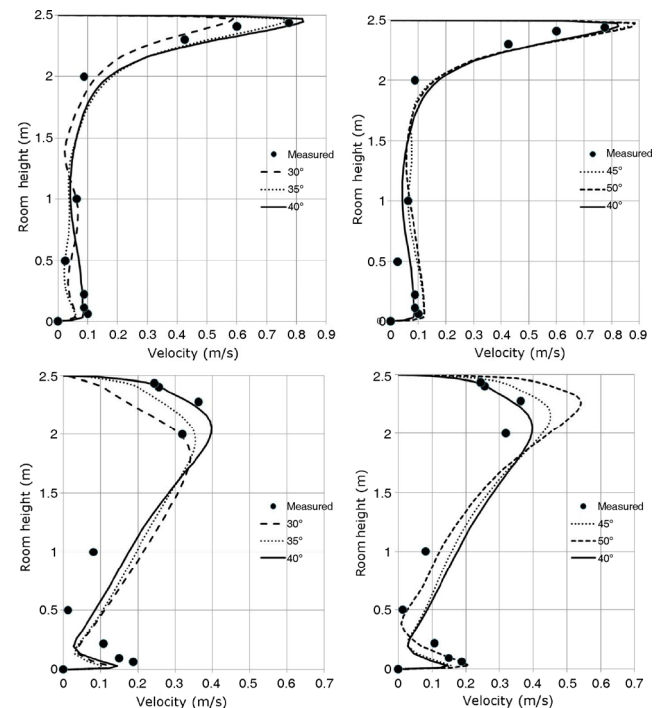


Fig. 5 Comparison of velocity profiles for different jet angles with measured data at  $x = 1.4$  m (top) and  $3$  m (bottom)

important in room air simulations. A diffuser inlet angle of  $40^\circ$  was used for the rest of the study.

## 4.4 Effect of reduced diffuser flow rates

The diffuser flow rates were reduced down to 15% of the design flow rate in order to study the jet momentum, draft, and temperature distribution inside the room. The heat gain from the external window and outside walls of the office room was reduced accordingly such that, the return air temperature was approximately constant as it would be with a constant thermostat setpoint. The inlet temperature was maintained constant at 15 °C. Flow rates at 50%, 40%, 30%, 20%, and 15% of the design flow rate were tested. However, only the results for 50%, 30%, and 15% are presented in this paper for brevity. The temperature profile is plotted for the symmetry plane in the center of the room.

#### 4.4.1 15% of diffuser design flow rate

The reduction of the diffuser flow rate to 15% of the design flow rate was the lowest flow rate case. Figure 6 shows the path lines of air particles released from the diffuser outlet. The figure indicates that due to lowered jet momentum, the cold air did not attach itself to the ceiling and fell directly down to only one side of the room, not mixing with the rest of the air in the room. This phenomenon is called “dumping” of the cold jet. The jet drop is further shown in Fig. 7, where the contours of temperature are plotted in the symmetry plane in the room. The temperature in the occupied zone, immediately below the diffuser, was at 18 °C, whereas it was maintained almost at 20.5 °C in the other regions of the room.

Figure 7 shows that in the symmetry plane at  $x = 0.25$  m (where the cold jet falls into the occupied zone) the temperature varies from 19 to 20.25 °C. The temperature values along the near wall region were almost constant along the lengthwise direction of the room; this was due to

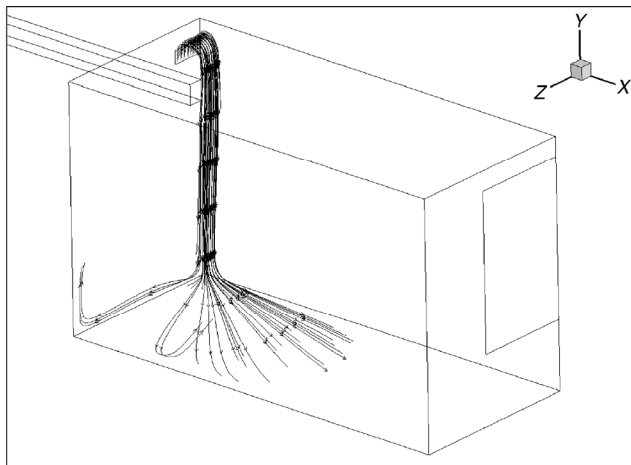


**Fig. 6** Isometric view of the path lines of particles released from the diffuser at 15% of the design flow rate

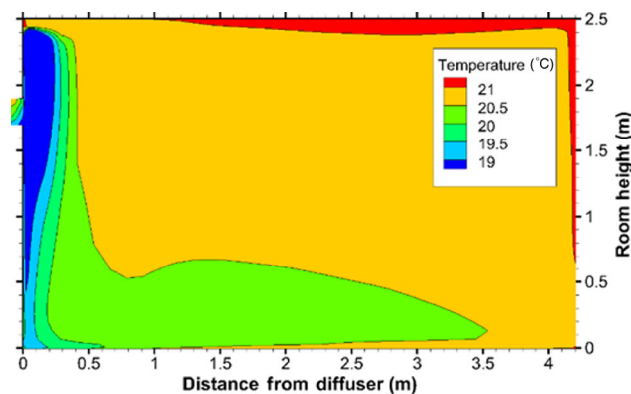


**Fig. 7** Contours of air temperature in the symmetry plane at 15% of the design flow rate

the cold jet not entering this region. High temperatures of air in the near wall plane were due to the direct heat gain from the walls of the room. Hence, a person standing just below the diffuser would feel the cold jet draft hitting directly on his head whereas a person standing near the window or wall would not feel the low temperatures at all.

#### 4.4.2 30% of diffuser design flow rate

The diffuser flow rate was altered to 30% of the design flow rate and the thermal loading was adjusted accordingly. The path lines and temperature variation in the symmetry plane are shown in Fig. 8 and Fig. 9. The jet attached itself to the ceiling until  $x = 1.5$  m (due to the Coanda effect) and then dropped into the occupied zone. The jet spread was broader as compared to the previous case.

From Fig. 9, it was observed that the temperature near the ceiling varied from 18 to 22 °C along the length of the room but there was a maximum of 1 °C variation near head level (at  $y = 1.8$  m). The influence of dumping was not

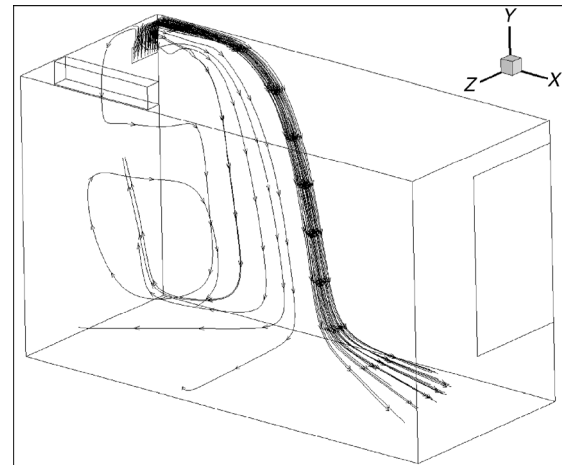


**Fig. 8** Isometric view of the path lines of particles released from the diffuser at 30% of the design flow rate

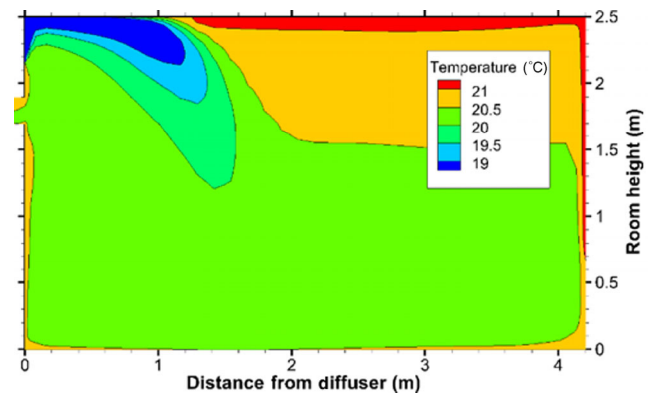


**Fig. 9** Contours of temperature in the symmetry plane at 30% of the design flow rate

considerable in the occupied zone. The temperature was low at  $x = 1.5$  m (as compared with the other locations of the room in lengthwise direction) because the jet entered the occupied zone near this pole.

#### 4.4.3 50% of diffuser design flow rate

The diffuser flow rate was then adjusted to 50% of the design flow rate, which is common for variable air volume units. The path lines plot (Fig. 10) and temperature contour plot (Fig. 11) show that the jet was attaching itself to half of the ceiling length and then diffused towards the wall at the opposite end. The primary jet air was not directly entering into the occupied zone until near the window. Overall, the temperatures in the occupied zone were maintained within 1 °C.

### 4.5 Thermal comfort results

The thermal comfort in terms of a percentage dissatisfied

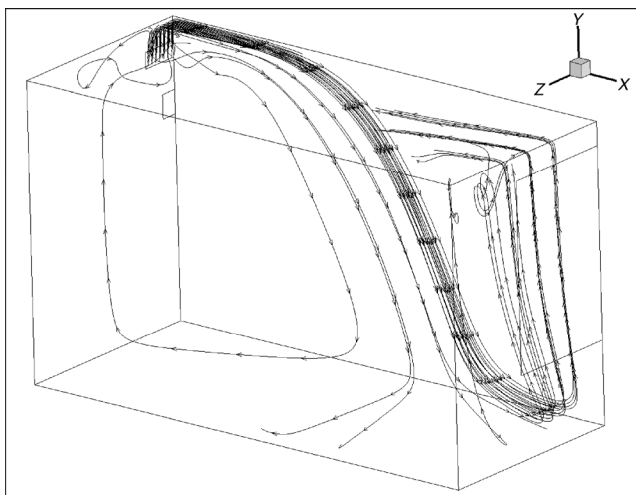


**Fig. 10** Isometric view of the path lines of particles released from the diffuser at 50% of the design flow rate

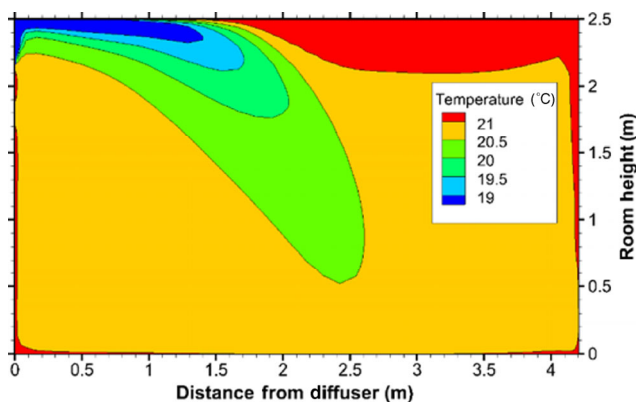


**Fig. 11** Contours of temperature (°C) in the symmetry plane at 50% of the design flow rate

(PD) index was calculated based on Fanger's comfort equation, Eq. (1). The necessary velocity, temperature, and turbulence intensity values were taken on the symmetry plane. At 15% of the diffuser flow rate, the percent dissatisfaction is below 5% for the majority of the room, except for the area directly below the diffuser. The cold supply air is dumped directly below the diffuser resulting in a percent dissatisfaction percentage greater than 25% in the occupied zone directly below the diffuser.

The entire occupied zone has a percent dissatisfaction percentage below 15% in the 30% of design diffuser flow rate case. The percentage of dissatisfaction increases when the flow rate is increased further to 50% of the design diffuser flow rate. This is due to the differences in velocity, not the space temperature. The overall temperature in the modeled occupied zone was higher for the 50% case than for the 30% case, which would decrease the percent dissatisfied according to Eq. (1). However, the increase in velocity offsets the higher temperature and increases the percent dissatisfaction for the 50% case as seen in Fig. 12.

### 5 Conclusions and implications for VAV minimum flow settings

The jet momentum, draft, and temperature distribution inside the room were numerically studied to examine the impact of reduced flow rates on thermal comfort. This study first validated CFD simulation results with measured data to establish the accuracy of the simulation results. For the CFD modeling of the supply diffuser, the turbulence model had a considerable impact on calculated room air velocities for the same grid size and boundary conditions. Hence, selection of the appropriate turbulence model is important for the result accuracy levels. The transition k-kl-w turbulence model performed best for the simulations in this room air. This study also found that a radiation model should be incorporated in CFD simulations for more accurate predictions of room air temperatures. Finally, the jet momentum was sensitive to different diffuser inlet angles (in the range of  $\pm 10^\circ$ ). Proper care should be taken for specifying the inlet angle. Simulation results should be validated with measured data.

The validated CFD model provided an opportunity to reduce the supply flow rates from 100% for the design flow to 15% for the worst scenario case. For the worst scenario case, the mixing of cold air with the warm room air was reduced, and the cold jet fell directly into the occupied zone. This caused the air temperatures where the jet fell to be as much as 2 °C lower than the rest of the room. At a flow rate equal to 30% of the design flow rate, there was a difference of 1 °C in the vertical direction where the jet fell



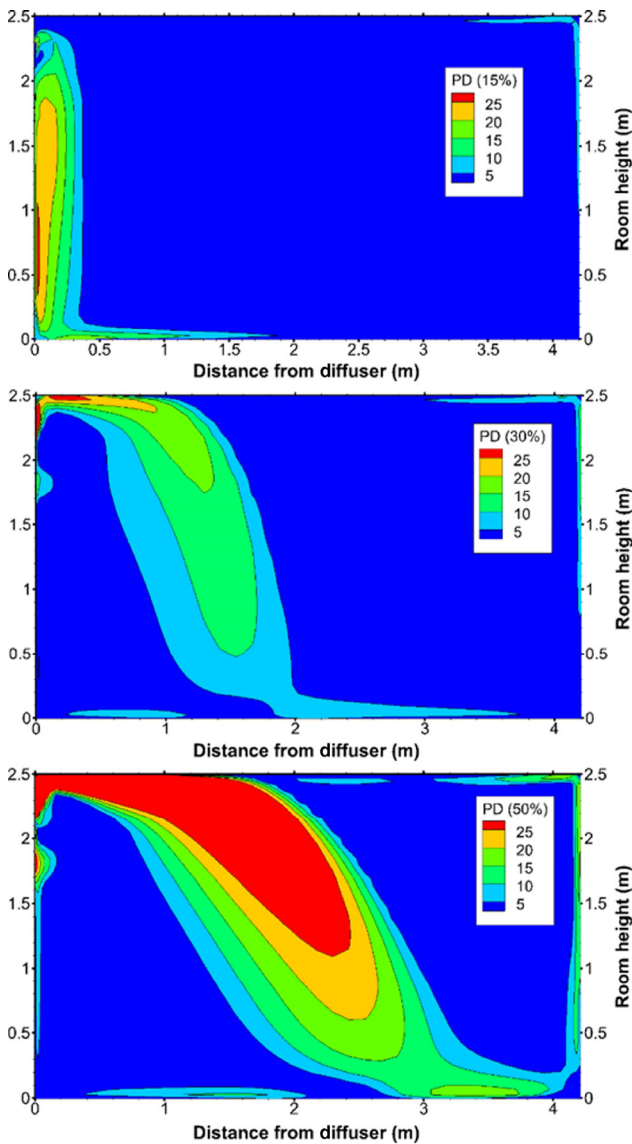


Fig. 12 Percentage dissatisfied at 15%, 30%, and 50% of design flow rate along the symmetry plane

into the occupied zone, but in other parts of the room, the temperature distribution was constant in the vertical direction of the occupied space.

The percent dissatisfaction at 1 m room height was greater than 25% for the lowest diffuser flow rate tested (15% of the design flow rate) directly under the diffuser, which was the highest of the test cases. However, it was no higher than 5% throughout more than 90% of the room at this flow rate. In contrast, at the higher flow rates, the increased velocity made a larger portion of the room feel more uncomfortable than the lowest diffuser flow rate case. In contrast, at the higher flow rates, the percent dissatisfied index was 5% or less in only 60%–80% of the room due to increased velocity.

Evidence of dumping was already found at the traditional

minimum flow rate setting of 30% of design, and so there would be little harm in reducing the minimum flow rate further. Reducing the flow rate below 30% of design just moved the location of the dumping closer to the diffuser. For very low diffuser flow rates (below 30% of the design flow rate), it is recommended that desks be placed away from the supply diffuser to avoid discomfort. Overall, the simulation results indicate that uniform temperatures are maintained in the room at flow rates as low as 15% of design except immediately under the diffuser. This suggests that the VAV minimum flow rates can be set below 30% of design flow as long as the diffuser is at least 1 m from an occupant's position. This conclusion agrees with the results of ASHRAE RP-1515, which suggests that significant energy savings result from reducing the minimum flow rates with little concern for increases in thermal discomfort.

## Appendix

The CFD software employed had the variables for velocity magnitude, temperature, and turbulence intensity available. Table A1 shows example calculations for Fanger's comfort equation for the 30% of diffuser design flow rate case along one line, specifically at a room height of 1.5 m along the symmetry plane. Figure 12 shows the related surface plot for the symmetry plane.

Table A1 Sample calculations for percent dissatisfied from Fanger's equation (Eq. (1))

$x$ (m)	$y$ (m)	Velocity magnitude (m/s)	Temperature ( $^{\circ}$ C)	Turbulence intensity, $Tu$	Percent dissatisfied (%)
0.13	1.50	0.0327	20.45	0.0348	0.00
0.22	1.50	0.0444	20.44	0.0352	0.00
0.35	1.50	0.0520	20.43	0.0369	0.90
0.47	1.50	0.0624	20.41	0.0393	2.80
0.60	1.50	0.0755	20.37	0.0423	4.40
0.72	1.50	0.0913	20.32	0.0457	5.96
0.85	1.50	0.1100	20.25	0.0496	7.55
0.98	1.50	0.1316	20.16	0.0538	9.19
1.10	1.50	0.1578	20.05	0.0578	11.02
1.23	1.50	0.1878	19.91	0.0604	12.96
1.35	1.50	0.2085	19.82	0.0616	14.24
1.48	1.50	0.2048	19.84	0.0636	14.01
1.60	1.50	0.1661	20.01	0.0653	11.57
1.73	1.50	0.0894	20.30	0.0591	5.80
1.85	1.50	0.0376	20.44	0.0471	0.00
1.98	1.50	0.0221	20.48	0.0374	0.00
2.11	1.50	0.0201	20.49	0.0307	0.00
2.23	1.50	0.0203	20.49	0.0260	0.00

(Continued)

$x$ (m)	$y$ (m)	Velocity magnitude (m/s)	Temperature (°C)	Turbulence intensity, $Tu$	Percent dissatisfied (%)
2.36	1.50	0.0211	20.49	0.0228	0.00
2.48	1.50	0.0218	20.49	0.0207	0.00
2.61	1.50	0.0221	20.49	0.0196	0.00
2.73	1.50	0.0219	20.49	0.0191	0.00
2.86	1.50	0.0211	20.50	0.0190	0.00
2.98	1.50	0.0198	20.50	0.0190	0.00
3.11	1.50	0.0180	20.50	0.0190	0.00
3.23	1.50	0.0158	20.50	0.0191	0.00
3.36	1.50	0.0134	20.50	0.0191	0.00
3.49	1.50	0.0107	20.50	0.0190	0.00
3.61	1.50	0.0081	20.50	0.0188	0.00
3.74	1.50	0.0054	20.50	0.0185	0.00
3.86	1.50	0.0028	20.49	0.0181	0.00
3.99	1.50	0.0004	20.49	0.0182	0.00
4.09	1.50	0.0075	20.49	0.0217	0.00
4.15	1.50	0.0469	20.58	0.0302	0.00
4.18	1.50	0.1428	21.13	0.0269	9.26

## References

- ANSYS (2013). ANSYS Mechanical User's Guide.
- Arens E, Zhang H, Hoyt T, Kaam S, Goins J, Bauman F, Zhai Y, Webster T, West B, Paliaga G, Stein J, Seidl R, Tully B, Rimmer J, Toftum J (2012). Thermal and air quality acceptability in buildings that reduce energy by reducing minimum airflow from overhead diffusers. *ASHRAE RP-1515*.
- Arens E, Xu T, Miura K, Hui Z, Fountain M, Bauman F (1998). A study of occupant cooling by personally controlled air movement. *Energy and Buildings*, 27: 45–59.
- ASHRAE (2013). Thermal environmental conditions for human occupancy. ANSI/ASHRAE Standard 55-2013.
- Cândido C, de Dear RJ, Lamberts R, Bittencourt L (2010). Air movement acceptability limits and thermal comfort in Brazil's hot humid climate zone. *Building and Environment*, 45: 222–229.
- Carlucci S, Pagliano L (2012). A review of indices for the long-term evaluation of the general thermal comfort conditions in buildings. *Energy and Buildings*, 53: 194–205.
- Charles KE (2003). Fanger's thermal comfort and draught models. National Research Council of Canada, IRC Research Report RR-162.
- Chen Q (1995). Comparison of different  $k-\epsilon$  models for indoor airflow computations. *Numerical Heat Transfer, Part B: Fundamentals*, 28: 353–369.
- Chen Q, Moser A (1991). Simulation of a multiple-nozzle diffuser. In: Proceedings of 12th AIVC Conference, Ottawa, Canada, pp. 1–14.
- Cheng Y, Niu J, Gao N (2012). Thermal comfort models: A review and numerical investigation. *Building and Environment*, 47: 13–22.
- Cheong KWD, Djunaedy E, Chua YL, Tham KW, Sekhar SC, Wong NH, Ullah MB (2003). Thermal comfort study of an air-conditioned lecture theatre in the tropics. *Building and Environment*, 38: 63–73.
- De Dear RJ, Akimoto T, Arens E, Brager G, Candido C, Cheong KWD, Li B, Nishihara N, Sekhar SC, Tanabe S, Toftum J, Zhang H, Zhu Y (2013). Progress in thermal comfort research over the last twenty years. *Indoor Air*, 23: 442–461.
- Djongyang N, Tchinda R, Njomo D (2010). Thermal comfort: A review paper. *Renewable and Sustainable Energy Reviews*, 14: 2626–2640.
- Ewert M, Renz U, Vogl N, Zeller M (1991). Definition of the flow parameters at the room inlet devices-measurements and calculations. In: Proceedings of 12th AIVC Conference, Ottawa, Canada, pp. 231–237.
- Fanger P, Melikov A, Hanzawa H, Ring J (1988). Air turbulence and sensation of draft. *Energy and Buildings*, 12: 21–39.
- Fanger P, Christensen N (1986). Perception of draught in ventilated spaces. *Ergonomics*, 29: 215–235.
- Fountain M, Bauman F, Arens E, Miura K, de Dear R (1994). Locally controlled air movement preferred in warm isothermal environments. *ASHRAE Transactions*, 100(2): 937–952.
- Gosman A, Nielsen P, Restivo A, Whitelaw J (1980). The flow properties of rooms with small ventilation openings. *Journal of Fluids Engineering*, 102: 316–323.
- Heikkinen J (1991a). Modeling of a supply air terminal for room airflow simulation. In: Proceedings of 12th AIVC Conference, Ottawa, Canada, pp. 213–230.
- Heikkinen J (1991b). Measurements of test cases B2, B3, E2, E3 (isothermal and summer cooling cases). IEA Annex 20 Research item 1.16 and 1.17.
- Huo Y, Zhang J, Shaw C, Haghight F (1996). A new method to describe boundary conditions in CFD simulation. In: Proceedings of International Conference on Air Distribution in Rooms (ROOMVENT), Yokohama, Japan, pp. 233–240.
- Kajiya R, Hiruta K, Sakai K, Ono H, Sudo T (2011). Thermal environment prediction using CFD with a virtual mannequin model and experiment with subject in a floor heating room. In: Proceedings of 12th International IBPSA Building Simulation Conference, Sydney, Australia, pp. 1670–1677.
- Kubo H, Isoda N, Enomoto-Koshimizu H (1997). Cooling effects of preferred air velocity in muggy conditions. *Building and Environment*, 32: 211–218.
- Kwong QJ, Adam NM, Sahari BB (2014). Thermal comfort assessment and potential for energy efficiency enhancement in modern tropical buildings: A review. *Energy and Buildings*, 68: 547–557.
- Lemaire AD, Chen Q, Ewert M, Heikkinen J, Inard C, Moser A, Nielsen PV, Whittle G (1993). Room air and contaminant flow, evaluation of computational methods. Subtask-1 Summary Report.

- Luo S, Heikkinen J, Roux B (2004). Simulation of airflow in the IEA annex 20 test room—Validation of a simplified model for the nozzle diffuser in isothermal test cases. *Building and Environment*, 39: 1403–1415.
- Mendell MJ, Mirer AG (2009). Indoor thermal factors and symptoms in office workers: Findings from the US EPA BASE study. *Indoor Air*, 19: 291–302.
- Nielsen PV (1992). The description of supply openings in numerical models for room air distribution. *ASHRAE Transactions*, 98(1): 963–971.
- Nielsen PV (1989). Representation of boundary conditions at supply openings. IEA Annex 20 Research Item No. 1.11.
- Noh K, Jang J, Oh M (2007). Thermal comfort and indoor air quality in the lecture room with 4-way cassette air-conditioner and mixing ventilation system. *Building and Environment*, 42: 689–698.
- Riachi Y, Clodic D (2014). A numerical model for simulating thermal comfort prediction in public transportation buses. *International Journal of Environmental Protection and Policy*, 2: 1–8.
- Rupp RF, Vásquez NG, Lamberts R (2015). A review of human thermal comfort in the built environment. *Energy and Buildings*, 105: 178–205.
- Simone A, Olesen BW, Stoops JL, Watkins AW (2013). Thermal comfort in commercial kitchens (RP-1469): Procedure and physical measurements (part 1). *HVAC&R Research*, 19: 1001–1015.
- Skovgaard M, Nielsen P (1991). Modeling complex inlet geometries in CFD applied to airflow in ventilated rooms. In: Proceedings of 12th AIVC Conference, Ottawa, Canada, pp. 183–200.
- Srebric J, Chen Q (2002). Simplified numerical models for complex air supply diffusers. *HVAC&R Research*, 8: 277–294.
- Srebric J, Chen Q (2001). A method of test to obtain diffuser data for CFD modeling of room airflow (RP-1009). *ASHRAE Transactions*, 107(2): 108–116.
- Srebric J (2000). Simplified methodology for indoor environment design. PhD Dissertation, Massachusetts Institute of Technology, USA.
- Stamou AI, Katsiris I, Schaelin A (2008). Evaluation of thermal comfort in Galatsi arena of the Olympics “Athens 2004” using a CFD model. *Applied Thermal Engineering*, 28: 1206–1215.
- Svidt K (1994). Investigation of inlet boundary conditions for numerical prediction of airflow in livestock buildings. Aalborg University, Indoor Environmental Technology, No. 38. Vol. R9407.
- Taleghani M, Tenpierik M, Kurvers S, van den Dobbelaars A (2013). A review into thermal comfort in buildings. *Renewable and Sustainable Energy Reviews*, 26: 201–215.
- Yang L, Yan H, Lam JC (2014). Thermal comfort and building energy consumption implications—A review. *Applied Energy*, 115: 164–173.
- Zhang H, Arens E, Fard SA, Huizenga C, Paliaga G, Brager G, Zagreus L (2007). Air movement preferences observed in office buildings. *International Journal of Biometeorology*, 51: 349–360.